BJP British Journal of Pharmacology

DOI:10.1111/bph.12458
www.brjpharmacol.org

RESEARCH PAPER

Loop diuretics are open-channel blockers of the cystic fibrosis transmembrane conductance regulator with distinct kinetics

Min Ju[1], Toby S Scott-Ward[1], Jia Liu[1], Pissared Khuituan[1,2], Hongyu Li[1], Zhiwei Cai[1], Stephen M Husbands[3] and David N Sheppard[1]

[1]*School of Physiology and Pharmacology, University of Bristol, Bristol, UK,* [2]*Center of Calcium and Bone Research, Department of Physiology, Faculty of Science, Mahidol University, Bangkok, Thailand, and* [3]*Department of Pharmacy and Pharmacology, University of Bath, Bath, UK*

Correspondence
David N Sheppard, School of Physiology and Pharmacology, University of Bristol, Medical Sciences Building, University Walk, Bristol BS8 1TD, UK.
E-mail:
d.n.sheppard@bristol.ac.uk

Author contributions: M Ju, TS Scott-Ward, J Liu and P Khuituan are co-first author.

Keywords
ATP-binding cassette transporter; CFTR; chloride ion channel; open-channel blockade; epithelial ion transport; loop diuretics; NKCC; bumetanide; furosemide; glibenclamide

Received
11 May 2013
Revised
21 September 2013
Accepted
26 September 2013

BACKGROUND AND PURPOSE

Loop diuretics are widely used to inhibit the Na^+, K^+, $2Cl^-$ co-transporter, but they also inhibit the cystic fibrosis transmembrane conductance regulator (CFTR) Cl^- channel. Here, we investigated the mechanism of CFTR inhibition by loop diuretics and explored the effects of chemical structure on channel blockade.

EXPERIMENTAL APPROACH

Using the patch-clamp technique, we tested the effects of bumetanide, furosemide, piretanide and xipamide on recombinant wild-type human CFTR.

KEY RESULTS

When added to the intracellular solution, loop diuretics inhibited CFTR Cl^- currents with potency approaching that of glibenclamide, a widely used CFTR blocker with some structural similarity to loop diuretics. To begin to study the kinetics of channel blockade, we examined the time dependence of macroscopic current inhibition following a hyperpolarizing voltage step. Like glibenclamide, piretanide blockade of CFTR was time and voltage dependent. By contrast, furosemide blockade was voltage dependent, but time independent. Consistent with these data, furosemide blocked individual CFTR Cl^- channels with 'very fast' speed and drug-induced blocking events overlapped brief channel closures, whereas piretanide inhibited individual channels with 'intermediate' speed and drug-induced blocking events were distinct from channel closures.

CONCLUSIONS AND IMPLICATIONS

Structure–activity analysis of the loop diuretics suggests that the phenoxy group present in bumetanide and piretanide, but absent in furosemide and xipamide, might account for the different kinetics of channel block by locking loop diuretics within the intracellular vestibule of the CFTR pore. We conclude that loop diuretics are open-channel blockers of CFTR with distinct kinetics, affected by molecular dimensions and lipophilicity.

Abbreviations

BHK cells, baby hamster kidney cells; CF, cystic fibrosis; CFTR, cystic fibrosis transmembrane conductance regulator; FRT cells, Fischer rat thyroid cells; i, single-channel current amplitude; I_{Cl}^{apical}, apical membrane Cl^- current; M, transmembrane segment; MSD, membrane-spanning domain; NKCC, Na^+, K^+, $2Cl^-$ co-transporter; NMDG, *N*-methyl-D-glucamine; P_o, open probability

Introduction

During transepithelial Cl^- secretion, the Na^+, K^+, $2Cl^-$ co-transporter isoform 1 (NKCC1; SLC12A2) (Delpire *et al.*, 1994; Haas and Forbush, 2000; Hebert *et al.*, 2004) actively accumulates Cl^- within epithelial cells across the basolateral membrane, whereas the cystic fibrosis transmembrane conductance regulator (CFTR; ABCC7) Cl^- channel (Riordan *et al.*, 1989; Holland *et al.*, 2003; Gadsby *et al.*, 2006) mediates the passive exit of Cl^- across the apical membrane (receptor and channel nomenclature follows Alexander *et al.*, 2013). High-affinity inhibitors of NKCC1 and CFTR are therefore valuable tools to identify these transport proteins, investigate transepithelial Cl^- transport mechanisms and treat disease (Russell, 2000; Sheppard, 2004). Loop diuretics, such as bumetanide and furosemide, are widely used to inhibit NKCC1 (Haas and Forbush, 2000). However, they are not selective blockers (Cabantchik and Greger, 1992). Interestingly, Reddy and Quinton (1999) demonstrated that bumetanide and furosemide inhibit salt reabsorption in native human sweat duct epithelia, a tissue with modest NKCC1 activity. These authors interpreted their data to suggest that loop diuretics inhibit salt reabsorption by blocking CFTR. Consistent with this idea, Venglarik (1997) reported that bumetanide and furosemide inhibit the single-channel activity of CFTR.

The chemical structures of bumetanide and furosemide show some similarities to that of glibenclamide, the best-studied CFTR blocker (Li and Sheppard, 2009). Therefore, we were interested to learn how loop diuretics inhibit CFTR. Our specific aims were, firstly, to understand the mechanism of CFTR inhibition and, secondly, to investigate the relationship between the chemical structures of loop diuretics and CFTR inhibition. We selected for study bumetanide, furosemide, piretanide and xipamide (Figure 1). These loop diuretics show a high degree of structural similarity, all being benzenesulfonamides with three further substituents on the aryl ring (Figure 1 and Supplementary Information Figure S1). Bumetanide and piretanide are very closely related, only differing in the 3-amino substituent (butylamino vs. pyrrolidino). Furosemide and xipamide differ from bumetanide and piretanide in substitution pattern (1,2,4,5-tetra substituted vs. 1,3,4,5-tetra substituted) and identity.

To investigate mechanisms of CFTR inhibition, we studied macroscopic and single-channel currents in excised inside-out membrane patches from cells expressing recombinant wild-type human CFTR. We found that loop diuretics are open-channel blockers that inhibit CFTR with similar

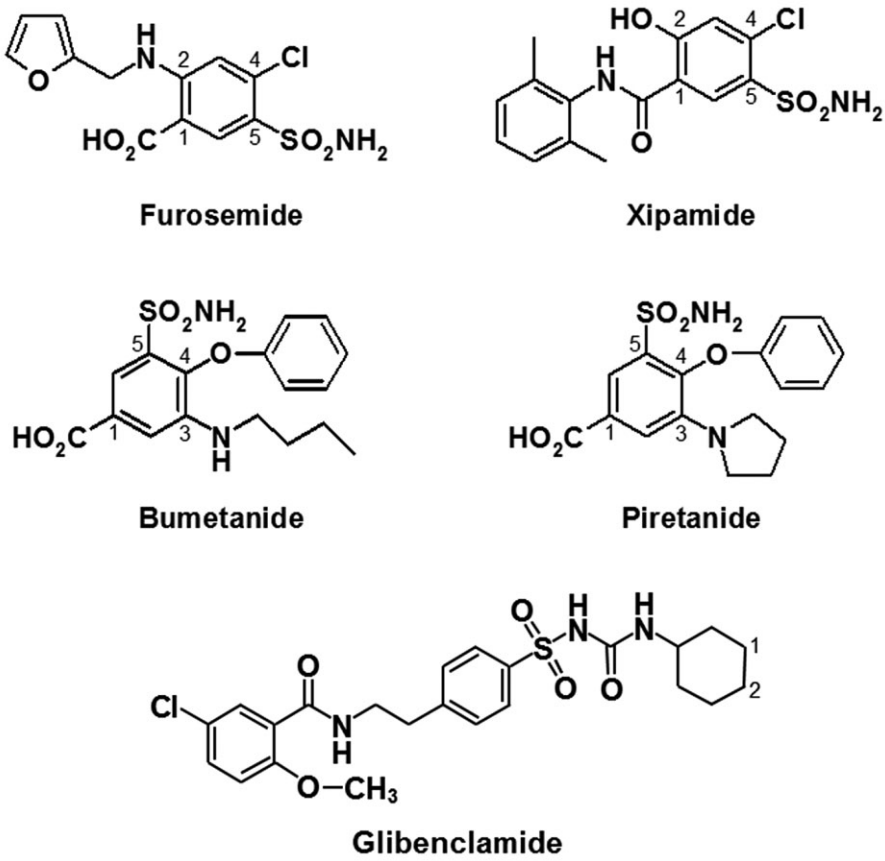

Figure 1

Chemical structures of loop diuretics. The structures of glibenclamide and the agents used in this study are shown. The 3-*cis* and 4-*trans* positions of the cyclohexyl ring of glibenclamide are indicated by the numbers 1 and 2 respectively. For further details, see the text.

potencies, but distinct kinetics; bumetanide and piretanide with 'intermediate' speed, and furosemide and xipamide with 'very fast' speed. Analysis of the chemical structures of loop diuretics suggests that the phenoxy group present in bumetanide and piretanide, but absent in furosemide and xipamide, might account for the different kinetics of channel block by locking loop diuretics within the intracellular vestibule of the CFTR pore. We conclude that differences in molecular dimensions and lipophilicity affect CFTR inhibition by loop diuretics.

Methods

Cells and cell culture

We used baby hamster kidney (BHK), Fischer rat thyroid (FRT) and mouse mammary epithelial (C127) cells stably expressing wild-type human CFTR (Marshall *et al.*, 1994; Farinha *et al.*, 2002; Zegarra-Moran *et al.*, 2002), as described previously (Sheppard and Robinson, 1997; Schmidt *et al.*, 2008). Cells were generous gifts from MD Amaral (University of Lisboa; BHK cells); LJV Galietta (Istituto Giannina Gaslini; FRT cells) and CR O'Riordan (Genzyme; C127 cells). C127 cells are the cell line of choice for single-channel studies of wild-type human CFTR because they express low levels of recombinant CFTR (e.g. Sheppard and Robinson, 1997). By contrast, BHK cells are preferred for measurements of macroscopic CFTR Cl^- currents because they express high levels of recombinant CFTR (e.g. Schmidt *et al.*, 2008). Because they form polarized epithelia with a high transepithelial resistance and because they lack expression of endogenous CFTR, FRT cells are the cell line of choice to investigate transepithelial Cl^- transport mediated by recombinant CFTR (Sheppard *et al.*, 1994). The single-channel behaviour of wild-type human CFTR in excised membrane patches from different mammalian cells is equivalent (Chen *et al.*, 2009).

Patch-clamp experiments

CFTR Cl^- channels were recorded in excised inside-out membrane patches using an Axopatch 200A patch-clamp amplifier and pCLAMP software (both from MDS Analytical Technologies, Union City, CA, USA) (Sheppard and Robinson, 1997). The pipette (extracellular) solution contained (mM): 140 *N*-methyl-D-glucamine (NMDG), 140 aspartic acid, 5 $CaCl_2$, 2 $MgSO_4$ and 10 *N*-tris[Hydroxymethyl]methyl-2-aminoethanesulphonic acid (TES), adjusted to pH 7.3 with Tris ($[Cl^-]$, 10 mM). The bath (intracellular) solution contained (mM): 140 NMDG, 3 $MgCl_2$, 1 CsEGTA and 10 TES, adjusted to pH 7.3 with HCl ($[Cl^-]$, 147 mM; free $[Ca^{2+}]$, $<10^{-8}$ M) and was maintained at 37°C. CFTR was activated, channel rundown was prevented and the effects of loop diuretics were tested as described previously for CFTR blockade by niflumic acid (Scott-Ward *et al.*, 2004).

For single-channel studies, we used membrane patches containing ≤3 active channels. To determine channel number, we used the maximum number of simultaneous channel openings observed during the course of an experiment (Cai *et al.*, 2006). To investigate the voltage and external Cl^- concentration dependence of channel block, we used voltage-ramp protocols to acquire current–voltage (I–V) relationships (Cai *et al.*, 2003). To explore the time dependence of blockade, we bathed membrane patches in symmetrical Cl^--rich solutions and stepped voltage first from 0 to –100 mV and then from –100 to +100 mV before returning to 0 mV; the duration of each voltage step was 250 ms. We averaged multiple current records (5–30) acquired in the absence and presence of drugs before subtracting basal currents with no active channels recorded in the absence of PKA (75 nM) and ATP (1 mM) to isolate macroscopic CFTR Cl^- currents.

We recorded, filtered and digitized data as described previously [macroscopic (Scott-Ward *et al.*, 2004); single-channel (Sheppard and Robinson, 1997)]. Time-course data were analysed and the relationship between drug concentration and CFTR inhibition was fitted to the Hill equation as described (Scott-Ward *et al.*, 2004). To investigate the time dependence of CFTR inhibition following a hyperpolarizing voltage step, exponential functions were fit to current relaxations; capacitance transients were excluded from these fits. To measure single-channel current amplitude (i), Gaussian distributions were fit to current amplitude histograms. For open probability (P_o) and kinetic analyses, lists of open and closed times were created and dwell-time histograms were constructed, fitted and statistically tested as previously described (Winter *et al.*, 1994; Sheppard and Robinson, 1997). Only membrane patches that contained a single-active CFTR Cl^- channel were used for kinetic analyses.

Ussing chamber studies

We measured CFTR-mediated apical membrane Cl^- current (I_{Cl}^{apical}) in FRT epithelia after permeabilizing the basolateral membrane with nystatin as described previously (Li *et al.*, 2004).

Data analysis

Results are expressed as means ± SEM of *n* observations. To compare sets of data, we performed either an ANOVA or Student's *t*-test using SigmaStat™ (Systat Software Inc., Richmond, CA, USA). Differences were considered statistically significant when $P < 0.05$.

Materials

Unless specified, chemicals were purchased from the Sigma-Aldrich Company Ltd. (Gillingham, UK). Xipamide and piretanide were generous gifts of Dishman Europe Ltd. (London, UK) and Sanofi-Aventis Deutschland GmbH (Frankfurt am Main, Germany) respectively. Genistein was obtained from LC Laboratories (Woburn, MA, USA), $CFTR_{inh}$-172 from Calbiochem (Merck Chemicals Ltd., Nottingham, UK) and PKA purified from bovine heart was from Promega UK (Southampton, UK) or Calbiochem.

ATP was dissolved in intracellular solution, forskolin in methanol and all other reagents in DMSO. Stock solutions were stored at –20°C, with the exception of ATP, which was prepared directly before each experiment. Immediately before use, stock solutions were diluted to achieve final concentrations and, where necessary, the pH of the intracellular solution was readjusted to pH 7.3 to avoid pH-dependent changes in CFTR function (Chen *et al.*, 2009). DMSO did not affect CFTR activity (Sheppard and Robinson, 1997).

Results

Loop diuretics inhibit CFTR Cl^- currents

In this study, we investigated how the loop diuretics, bumetanide, furosemide, piretanide and xipamide, inhibit CFTR. Inspection of their chemical structures identifies a number of features, which could influence channel block (Figure 1; Li and Sheppard, 2009). All are large, organic anions, each possesses a benzenesulfonamide moiety, and with the exception of xipamide, each possesses a carboxyl group. Because the chemical structures of loop diuretics show some similarities to that of glibenclamide, the best-studied CFTR blocker (Figure 1), we compared the effects of loop diuretics with that of glibenclamide.

To investigate loop diuretic inhibition of CFTR, we studied CFTR Cl^- currents in excised inside-out membrane patches from C127 cells expressing wild-type human CFTR. Following CFTR activation, we added increasing concentrations of loop diuretics (10–250 μM) to the intracellular solution in the continuous presence of PKA (75 nM) and ATP (0.3 mM) and monitored current inhibition (Figure 2). For each loop diuretic, the relationship between drug concentration and current inhibition at –50 mV was well fitted by the Hill equation [furosemide: drug concentration causing half-maximal inhibition (K_i) = 71.24 ± 15.08 μM, Hill coefficient (n) = –1.07 ± 0.19; xipamide: K_i = 45.03 ± 3.51 μM, n = –0.78 ± 0.07; bumetanide: K_i = 55.58 ± 10.68 μM, n = –1.04 ± 0.10; piretanide: K_i = 57.73 ± 17.62 μM, n = –1.00 ± 0.07; n = 5 for all values; Figure 2]. When tested at lower concentrations, neither furosemide nor piretanide inhibited significantly CFTR [furosemide (1 μM), $I_{Drug}/I_{Control}$ = 92.7 ± 2.6%; piretanide (1 μM), $I_{Drug}/I_{Control}$ = 96.3 ± 1.8%; n = 6 for both; P > 0.1]. Channel blockade by loop diuretics was readily reversible (Figure 2A and C; data not shown). Two conclusions can be drawn from these data: firstly, loop diuretics interact with single site(s) on CFTR; and secondly, they inhibit CFTR with similar potency, which approaches that of glibenclamide (K_i = 36 ± 3 μM, n = –1.1 ± 0.1; n = 6; Sheppard and Robinson, 1997, see also Schultz *et al.*, 1996).

Time dependence following a hyperpolarizing voltage step distinguishes channel blockade by furosemide and piretanide

In preliminary studies (see the Supporting Information Results), we applied noise analysis to macroscopic currents (e.g. Venglarik *et al.*, 1996; Gong *et al.*, 2002; Scott-Ward *et al.*, 2004). In the presence of furosemide and xipamide, but not bumetanide and piretanide, a loop diuretic-induced Lorentzian component was observed (Supporting Information Figure S2; Supporting Information Table S1). These data suggest that the kinetics of CFTR inhibition by bumetanide and piretanide are slower than those of furosemide and xipamide. To explore this idea further, we investigated the time dependence of macroscopic current inhibition because CFTR

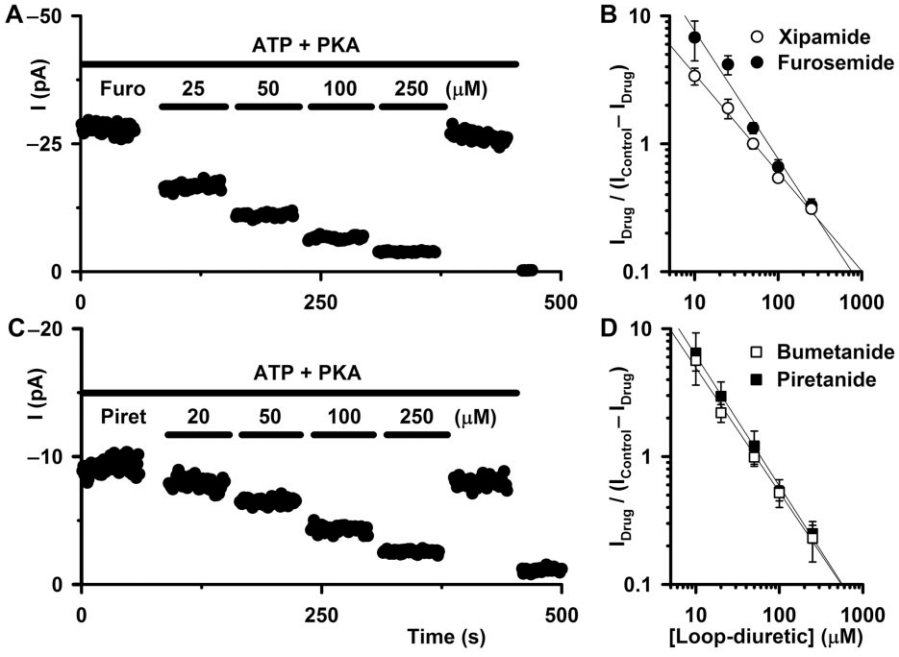

Figure 2

Loop diuretics inhibit CFTR. (A, C) Time courses of CFTR Cl^- current in excised inside-out membrane patches from C127 cells expressing wild-type human CFTR. During the periods indicated by the bars, ATP (0.3 mM), PKA (75 nM) and either furosemide (furo; 25–250 μM) or piretanide (piret; 20–250 μM) were present in the intracellular solution. Unless otherwise indicated, in this and subsequent figures, voltage was –50 mV and there was a large Cl^- concentration gradient across the membrane patch ($[Cl^-]_{internal}$ = 147 mM; $[Cl^-]_{external}$ = 10 mM). For the purpose of illustration, the time courses have been inverted so that upward deflections represent inward current. (B, D) Hill plots of CFTR inhibition by loop diuretics. Data are means ± SEM (n = 5). The continuous lines are the fits of first-order regression to the data (furosemide, r^2 = 0.98; xipamide, r^2 = 0.99; bumetanide, r^2 = 0.99; piretanide, r^2 = 1.00).

blockade by some agents (e.g. glibenclamide), but not by others (e.g. tolbutamide), leads to current relaxation following a hyperpolarizing voltage step (Zhou *et al.*, 2002; Zhang *et al.*, 2004a; Cui *et al.*, 2012). We selected for study furosemide and piretanide.

Figure 3A, D and G–I demonstrates that CFTR inhibition by furosemide (100 μM) is time independent following a hyperpolarizing voltage step. Over the duration of a 250 ms voltage step from 0 to –100 mV in the presence of furosemide (100 μM), there was no change in the magnitude of channel

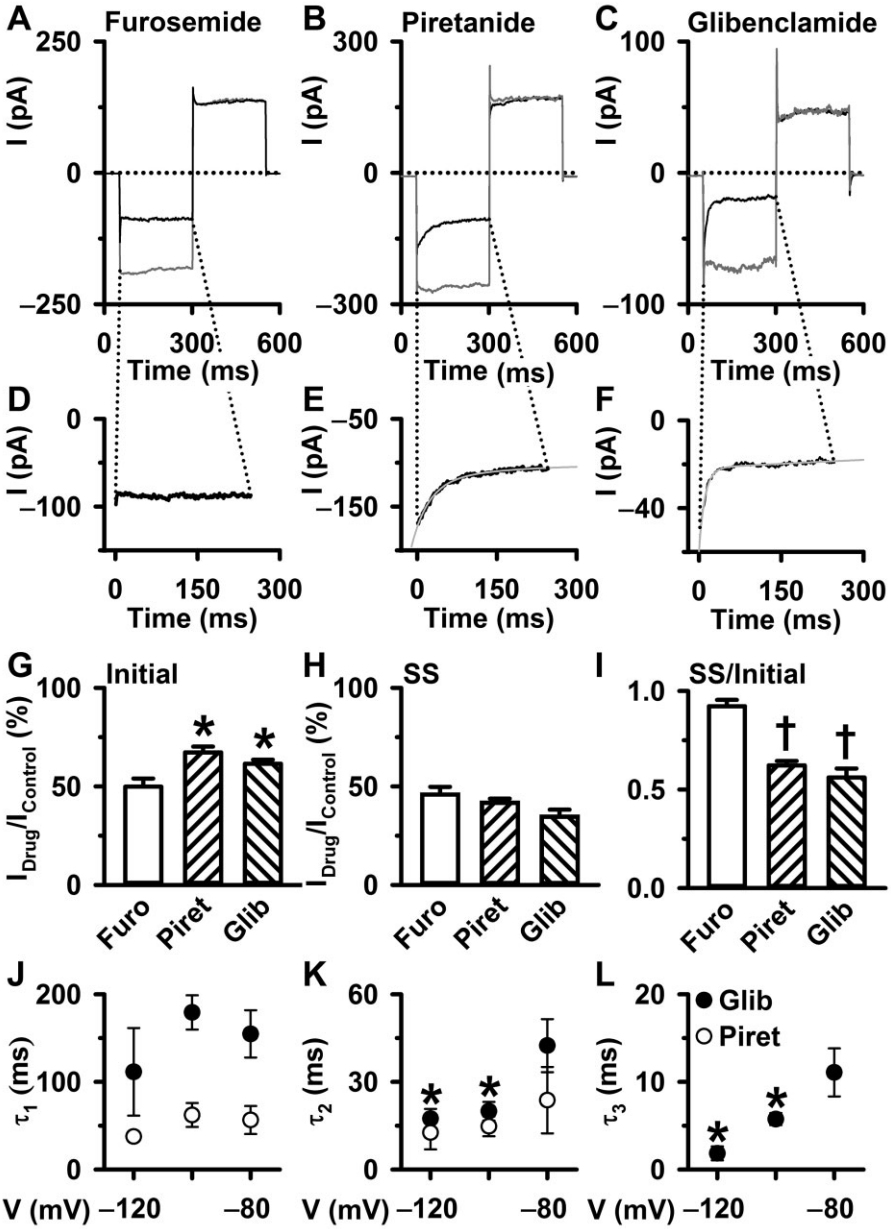

Figure 3

Time dependence of CFTR inhibition following a voltage step. (A–C) CFTR Cl^- currents recorded with (black) and without (grey) furosemide (100 μM), piretanide (100 μM) or glibenclamide (glib; 50 μM) by stepping voltage first from 0 to –100 mV and then from –100 to +100 mV before returning to 0 mV; holding voltage was 0 mV and voltage steps were 250 ms in duration. The data were acquired using membrane patches excised from BHK cells expressing wild-type human CFTR bathed in symmetrical 147 mM Cl^- solutions. ATP (1 mM) and PKA (75 nM) were continuously present in the intracellular solution. Dotted lines indicate zero current. (D–F) Higher resolution recordings of currents acquired at –100 mV in the presence of furosemide, piretanide and glibenclamide from the experiments shown in A–C. The grey continuous lines show the fit of exponential functions. (G–I) Fraction of current remaining at the start (initial) and end (steady state; SS) of voltage step and the ratio of the current remaining. Data are means + SEM ($n = 4$–6); *$P < 0.05$ versus furosemide; †$P < 0.001$ versus furosemide. (J–L) Voltage dependence of time constants fit to current relaxations in the presence of piretanide (100 μM) and glibenclamide (50 μM). The piretanide and glibenclamide data were fit with two- and three-component exponential functions respectively. Data are means ± SEM (piretanide, $n = 3$; glibenclamide, $n = 5$); *$P < 0.05$ versus glibenclamide data at –80 mV.

blockade (Figure 3A and D). The initial fraction of current remaining was similar to that at steady state, and hence, the current ratio for furosemide was close to 1 (Figure 3G–I). By contrast, CFTR inhibition by piretanide (100 μM) was time dependent following a hyperpolarizing voltage step like that of glibenclamide (50 μM) (Figure 3B, C and E–I). During a 250 ms voltage step from 0 to –100 mV in the presence of either blocker, current relaxed to a steady-state value; relaxation was smooth for piretanide, but sharp for glibenclamide (Figure 3B, C, E and F). For both piretanide and glibenclamide, the initial fraction of current remaining was ~30% greater than that at steady state, and hence, the current ratio for both blockers was about 0.6 (Figure 3G–I).

Consistent with previous results (Zhang *et al.*, 2004a; Cui *et al.*, 2012), Figure 3C demonstrates that there was substantially less current relaxation when membrane voltage was stepped from –100 to +100 mV in the presence of glibenclamide (50 μM) to elicit channel unblocking. Figure 3B shows similar results for piretanide (100 μM) when voltage was stepped from –100 to +100 mV; relief of piretanide blockade at +100 mV was rapid in marked contrast to the slow development of block when voltage was stepped from 0 to –100 mV. However, Figure 3A demonstrates that for furosemide (100 μM), there was no marked asymmetry between the onset and relief of block following voltage steps; both were time independent.

To understand better the time dependence of block development for piretanide and glibenclamide following a hyperpolarizing voltage step, we fitted exponential functions to current relaxations at –80, –100 and –120 mV. Two time constants were required to fit the piretanide data and three the glibenclamide data (Figure 3J–L). For both piretanide and glibenclamide, the slow time constant was voltage independent, but the faster time constants were voltage dependent, slowing with membrane depolarization (Figure 3J–L). We conclude that furosemide and piretanide inhibit macroscopic CFTR Cl^- currents with distinct kinetics, with those of piretanide resembling glibenclamide blockade of CFTR (Zhang *et al.*, 2004a).

Furosemide and piretanide inhibit single channels with distinct kinetics

To understand better how loop diuretics inhibit CFTR, we studied single channels. Figures 4 and 5 demonstrate that furosemide and piretanide markedly altered CFTR gating. The gating behaviour of wild-type human CFTR is characterized by bursts of channel openings interrupted by brief, flickery closures and separated by longer closures between bursts (Figures 4A and 5A). Furosemide (100 μM)-induced blocking events were very brief, with the result that the frequency of flickery closures interrupting bursts of channel openings increased markedly (Figure 4A). To quantify channel block, we measured i and P_o. Furosemide (100 μM) caused a small reduction in i (17%; $P < 0.05$), but a large decrease in P_o (59%; $P < 0.05$) (Figure 4B and C).

In the presence of piretanide (100 μM), bursts of channel openings were interrupted by many drug-induced blocking events (Figure 5A). Piretanide (100 μM) decreased markedly P_o (54%; $P < 0.05$), but was without effect on i ($P = 0.95$) (Figure 5B and C). Thus, consistent with the time dependence of channel block following a hyperpolarizing voltage step,

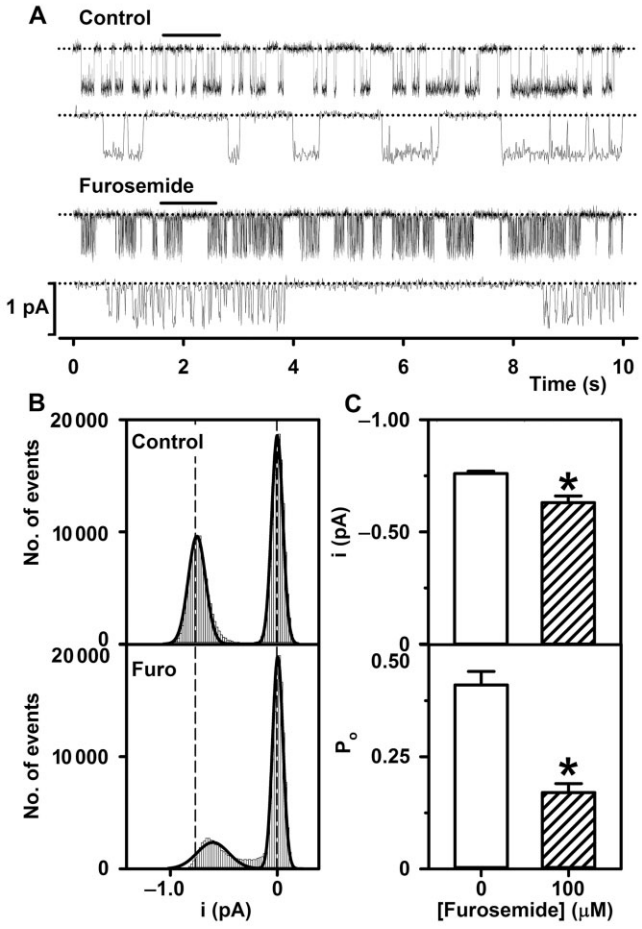

Figure 4

Furosemide block of individual CFTR Cl^- channels. (A) Representative recordings show the effects of furosemide (100 μM) on a single CFTR Cl^- channel in an excised inside-out membrane patch from a C127 cell expressing wild-type human CFTR. ATP (0.3 mM) and PKA (75 nM) were continuously present in the intracellular solution. Dotted lines indicate the closed-channel state and downward deflections channel openings. Beneath each prolonged 10 s recordings, 1 s portions indicated by the bars are shown on an expanded time scale. (B) Single-channel current amplitude histograms in the absence and presence of furosemide (100 μM) from the experiment shown in A. The continuous lines are the fit of Gaussian distributions to the data. The vertical dashed lines indicate the positions of the open and closed channels under control conditions; the closed-channel amplitude is shown on the right. (C) Effects of furosemide (100 μM) on i (top) and P_o (bottom). Data are means + SEM ($n = 6$); *$P < 0.05$ versus the control.

furosemide and piretanide have distinct effects on the single-channel activity of CFTR. Moreover, the effects of piretanide, but not furosemide, resemble those of glibenclamide (Schultz *et al.*, 1996; Sheppard and Robinson, 1997).

Furosemide and piretanide alter the dwell-time distributions of CFTR

To determine how furosemide and piretanide decreased P_o, we investigated gating kinetics using membrane patches that

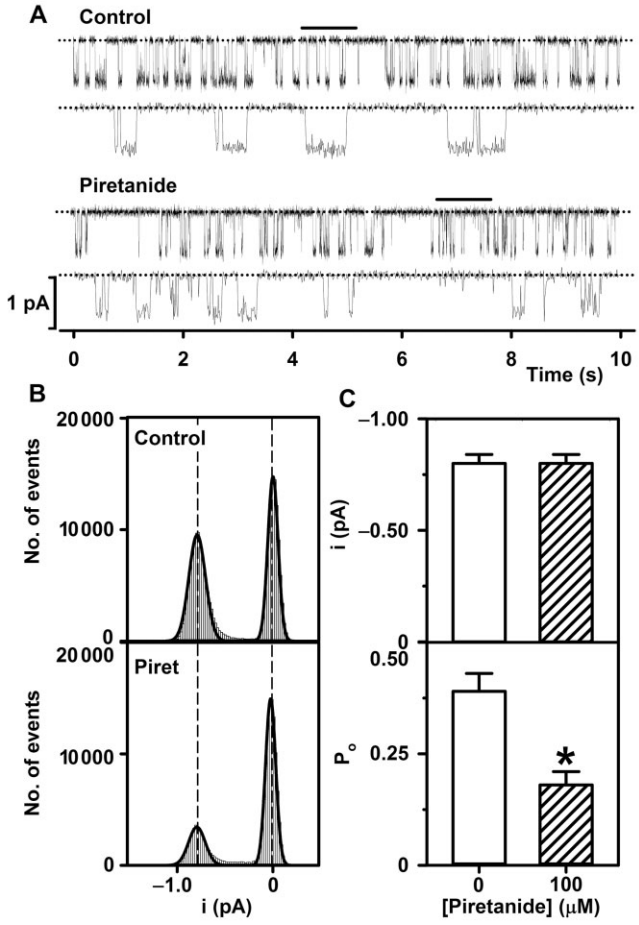

Figure 5

Piretanide block of individual CFTR Cl^- channels. (A) Representative recordings show the effects of piretanide (100 μM) on a single CFTR Cl^- channel in an excised inside-out membrane patch from a C127 cell expressing wild-type human CFTR. ATP (0.3 mM) and PKA (75 nM) were continuously present in the intracellular solution. Beneath each prolonged 10 s recordings, 1 s portions indicated by the bars are shown on an expanded time scale. (B) Single-channel current amplitude histograms in the absence and presence of piretanide (100 μM) from the experiment shown in A. (C) Effects of piretanide (100 μM) on i (top) and P_o (bottom). Data are means + SEM ($n = 6$); *$P < 0.05$ versus the control. Other details as in Figure 4.

contained only a single active channel. Consistent with previous results (e.g. Winter *et al.*, 1994), the open- and closed-time histograms of wild-type human CFTR were best fitted with one- and two-component exponential functions, respectively, described by the time constants τ_{O2}, τ_{C1} and τ_{C3} (Figure 6A and C; Supporting Information Table S2).

Like meglitinide (Cai *et al.*, 1999), in the presence of furosemide (100 μM), open- and closed-time histograms were best fitted with one- and two-component exponential functions, respectively (Figure 6B; Supporting Information Table S2); furosemide-induced blocking events could not be distinguished clearly from brief closures interrupting channel openings. Furosemide (100 μM) decreased the open-time constant (τ_{O2}) by 12.5-fold (Figure 6B; Supporting Information Table S2). It increased the fast closed-time constant (τ_{C1}) by 1.4-fold, while this time constant's share of the closed-time distribution expanded to 95% (Figure 6B; Supporting Information Table S2). However, furosemide (100 μM) was without effect on the slow closed-time constant (τ_{C3}), although this time constant's share of the closed-time distribution decreased to 5% (Figure 6B; Supporting Information Table S2).

In the presence of piretanide (100 μM), open and closed times were best fitted with two- and three-component exponential functions respectively (Figure 6D; Supporting Information Table S2). The new population of open times was described by a fast open-time constant (τ_{O1}), whereas the new population of closed times was described by an intermediate closed-time constant (τ_{C2}) (Figure 6D; Supporting Information Table S2). In addition, piretanide (100 μM) decreased τ_{O2} by 1.3-fold and τ_{C1} by 1.8-fold, but had little effect on τ_{C3} (Figure 6D; Supporting Information Table S2). The share of the closed-time distribution occupied by τ_{C1} decreased to 23%, whereas that occupied by τ_{C3} was unaffected (Figure 6D; Supporting Information Table S2). As a result, τ_{C2} occupied 45% of the closed-time distribution (Figure 6D; Supporting Information Table S2). Thus, with some differences in dwell-time duration, the effects of piretanide on CFTR gating kinetics are reminiscent of those of glibenclamide (Sheppard and Robinson, 1997).

The data in Figure 6 and Supporting Information Table S2 demonstrate that furosemide and piretanide decreased the open time of CFTR, suggesting that like glibenclamide (Sheppard and Robinson, 1997), they might be open-channel blockers of CFTR. Open-channel block of CFTR is described by the simple kinetic model:

$$C \underset{k_{close}}{\overset{k_{open}}{\leftrightarrow}} O \underset{k_{off}}{\overset{k_{on}[drug]}{\leftrightarrow}} B, \qquad (1)$$

where C, O and B represent the closed, open and blocked states of the channel, respectively; k_{open} and k_{close} are the transition rates for channel opening and closing; k_{on} is the second-order binding constant for drug binding to CFTR; and k_{off} is the first-order rate constant for drug dissociation from CFTR. The equilibrium dissociation constant for drug binding to CFTR, $K_d = k_{off}/k_{on}$; $k_{off} = 1/\tau_c$ and $k_{on} = (1/\tau_o) \times [drug]^{-1}$. For piretanide, using values of τ_{O1} and τ_{C2} from Supporting Information Table S2, we calculated values of $k_{on} = 1.67 \times 10^6\ M^{-1}{\cdot}s^{-1}$, $k_{off} = 156\ s^{-1}$ and $K_d = 89$ μM at –50 mV. Comparison of these data with those of glibenclamide ($k_{on} = 3.5 \times 10^6\ M^{-1}{\cdot}s^{-1}$, $k_{off} = 92\ s^{-1}$ and $K_d = 26$ μM; Sheppard and Robinson, 1997) reveals that glibenclamide is a more potent blocker than piretanide because it binds twofold faster and remains bound 40% longer.

Mechanism of loop diuretic inhibition of CFTR

CFTR is inhibited by open-channel and allosteric mechanisms (for review, see Li and Sheppard, 2009). To test whether loop diuretics are open-channel blockers of CFTR, we investigated the voltage dependence of macroscopic current blockade (Scott-Ward *et al.*, 2004). Under control conditions, CFTR Cl^- currents exhibited weak inward rectification (Figure 7A and B; Cai *et al.*, 2003). Consistent with our current relaxation data (Figure 3A and B), Figure 7A–D demonstrates that CFTR inhibition by both furosemide (100 μM) and piretanide

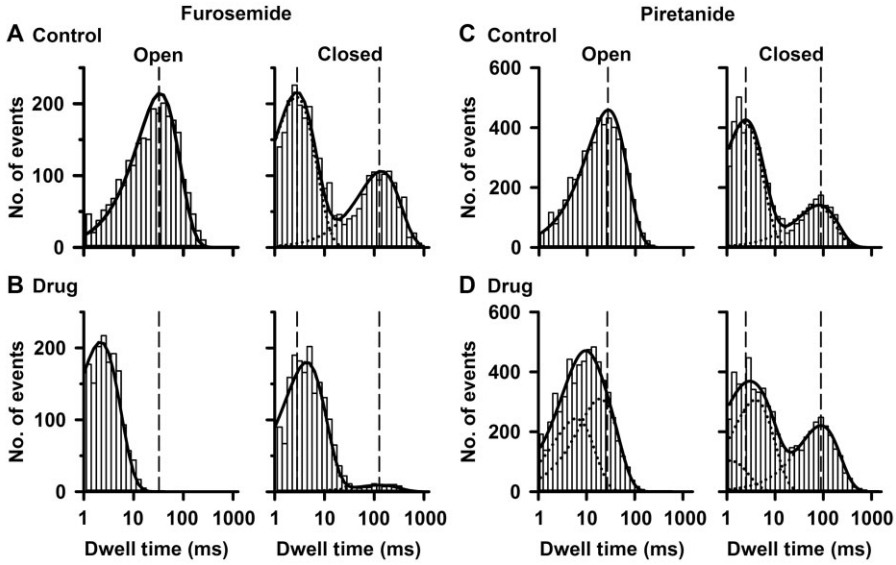

Figure 6

Dwell-time histograms of CFTR inhibited by furosemide and piretanide. Representative dwell-time histograms of single wild-type CFTR Cl^- channels recorded in the absence (A, C) and presence of either furosemide (100 μM; B) or piretanide (100 μM; D). Data are from experiments in which membrane patches, from C127 cells expressing wild-type human CFTR, contained only one active channel studied using the experimental conditions described in Figure 4. The continuous lines are the fit of one-, two- or three-component exponential functions to the data and the dotted lines show the individual components of these functions. The vertical dashed lines indicate mean values of the open- (τ_{O2}) and closed- (τ_{C1}, τ_{C3}) time constants under control conditions. Logarithmic x-axes, with 10 bins per decade, were used for dwell-time histograms.

(100 μM) is voltage dependent: at negative voltages, current magnitude was decreased strongly, whereas at positive voltages, inhibition was relieved robustly (piretanide) or current was augmented weakly above the control level (furosemide); enhancement of CFTR Cl^- current at positive voltages has been observed previously with some CFTR blockers [e.g. 5-nitro-2-(3-phenylpropylamino)-benzoic acid (NPPB); Wang *et al.*, 2005]. Using Equation (2), we calculated the voltage-dependent dissociation constant (K_d) for CFTR inhibition by furosemide and piretanide:

$$K_d(V) = [\text{drug}](I/I_o - I), \quad (2)$$

where $K_d(V)$ is the voltage-dependent dissociation constant at voltage V, and I and I_o are current values in the presence and absence of drug respectively. Figure 7E and F demonstrates that K_d values are voltage dependent and that furosemide is a weaker inhibitor than piretanide [furosemide, $K_d(0\text{ mV}) = 369 \pm 97$ μM ($n = 5$); piretanide, $K_d(0\text{ mV}) = 185 \pm 25$ μM ($n = 5$)]. However, both loop diuretics are weaker inhibitors than glibenclamide [$K_d(0\text{ mV}) = 37 \pm 6$ μM ($n = 5$); Sheppard and Robinson, 1997].

The electrical distance across the membrane sensed by blocking ions is calculated using the relationship (Woodhull, 1973):

$$K_d(V) = K_d(0\text{ mV})\exp[(-z'FV)/(RT)], \quad (3)$$

where z' is the apparent valency of the blocking ion [defined as the actual valency of the blocking ion (z) multiplied by the electrical distance across the membrane experienced by the blocking ion (δ)], and F, R and T are the Faraday constant, gas constant and absolute temperature respectively. Using the data in Figure 7E and F and assuming single binding sites for furosemide, $z' = 0.37 \pm 0.07$ ($n = 5$) and for piretanide, $z' = 0.25 \pm 0.04$ ($n = 5$), measured from the inside of the membrane. For comparison, for glibenclamide, $z' = 0.48 \pm 0.08$ ($n = 5$) (Sheppard and Robinson, 1997). While these data demonstrate that furosemide penetrates deeper into the transmembrane electric field than piretanide, comparison with glibenclamide is complicated because furosemide and piretanide possess two negative charges located on different parts of their structures, whereas glibenclamide has a single negative charge.

Next, we investigated whether Cl^- flow through the CFTR pore prevents macroscopic current blockade (Scott-Ward *et al.*, 2004). When the external Cl^- concentration was reduced to 10 mM by substituting Cl^- with the impermeant anion aspartate, the potency of furosemide inhibition was enhanced, whereas the electrical distance sensed was reduced (external $[Cl^-] = 147$ mM, $K_d(0\text{ mV}) = 369 \pm 97$ μM; $z' = 0.37 \pm 0.07$; $n = 5$; external $[Cl^-] = 10$ mM, $K_d(0\text{ mV}) = 136 \pm 23$ μM; $z' = 0.29 \pm 0.02$; $n = 6$; $P < 0.05$) (Figure 7E). However, piretanide inhibition of CFTR was unaffected (external $[Cl^-] = 147$ mM, $K_d(0\text{ mV}) = 185 \pm 25$ μM; $z' = 0.25 \pm 0.04$; external $[Cl^-] = 10$ mM, $K_d(0\text{ mV}) = 236 \pm 27$ μM; $z' = 0.18 \pm 0.02$; $n = 5$ for all values; $P > 0.11$) (Figure 7F). Thus, like glibenclamide (Sheppard and Robinson, 1997), furosemide, but not piretanide, might directly or indirectly compete with Cl^- for a common binding site within the CFTR pore.

CFTR blockade by some allosteric inhibitors is relieved by increasing the intracellular ATP concentration (Li and Sheppard, 2009). Supporting Information Figure S3 demonstrates that CFTR inhibition by furosemide (100 μM) and

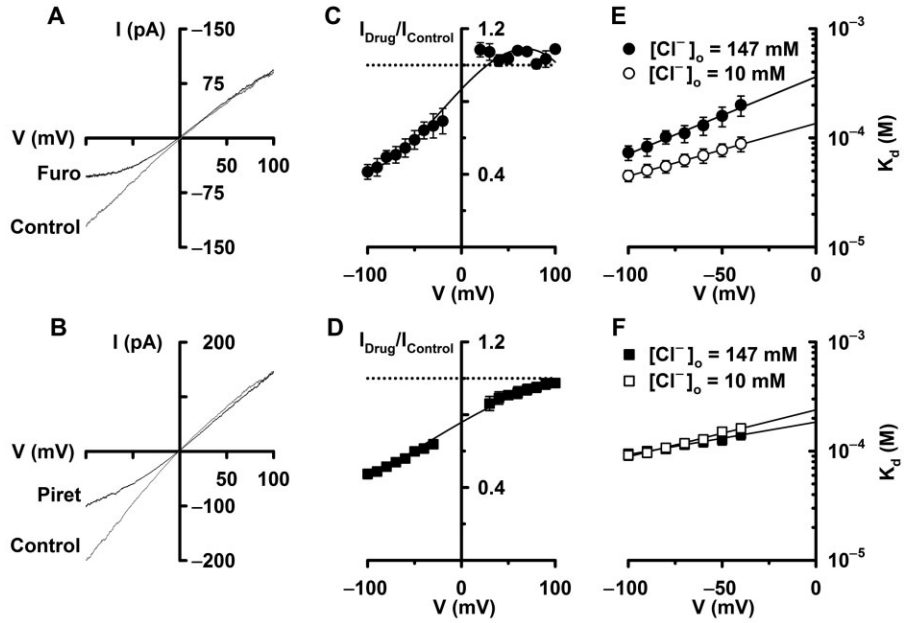

Figure 7

Voltage and external Cl^- concentration dependence of CFTR inhibition. (A, B) I–V relationships of CFTR Cl^- currents recorded in the absence and presence of furosemide (100 μM) and piretanide (100 μM), respectively, when membrane patches were bathed in symmetrical 147 mM Cl^- solutions. ATP (1 mM) and PKA (75 nM) were continuously present in the intracellular solution. (C, D) Effects of voltage on CFTR Cl^- current inhibition by furosemide (100 μM) and piretanide (100 μM). The continuous lines are the fit of sigmoidal curves with three parameters to the data. (E, F) Relationship between the voltage-dependent dissociation constant (K_d) and voltage for CFTR inhibition by furosemide and piretanide, respectively, when the external Cl^- concentration was either 147 or 10 mM. All data were acquired using BHK cells expressing wild-type human CFTR. In C–F, data are means ± SEM (n = 5–6) at each voltage. In E and F, the continuous lines are the fits of first order regressions to K_d values over the range −100 to −40 mV extrapolated to 0 mV (furosemide: $[Cl^-]_{external}$ = 147 mM, r^2 = 0.98; $[Cl^-]_{external}$ = 10 mM, r^2 = 0.99; piretanide: $[Cl^-]_{external}$ = 147 mM, r^2 = 0.98; $[Cl^-]_{external}$ = 10 mM, r^2 = 0.99).

piretanide (100 μM) was unaffected by raising the intracellular ATP concentration from 0.3 to 5 mM. This result suggests that like glibenclamide (Sheppard and Robinson, 1997), neither loop diuretic inhibits CFTR by interfering with ATP-dependent channel gating. However, some allosteric inhibitors interfere with CFTR gating without competing with ATP [e.g. GaTx1 (Fuller *et al.*, 2007); $CFTR_{inh}$-172 (Kopeikin *et al.*, 2010)], whereas other agents (e.g. thyroid hormones, Cai *et al.*, 2013) act at multiple steps within the CFTR gating pathway. Therefore, we investigated whether loop diuretic-blocked channels would first reopen before closing on washout of loop diuretic, PKA and ATP from the intracellular solution (see the Supporting Information Results and Scott-Ward *et al.*, 2004). Supporting Information Figure S4 demonstrates that on washout of furosemide, i returned to its control level before channels became quiescent. This suggests that furosemide accesses its binding site on CFTR from the open channel configuration.

Loop diuretics inhibit weakly CFTR Cl^- channels in the apical membrane of FRT epithelia

To evaluate the effects of loop diuretics on CFTR during transepithelial Cl^- transport, we studied CFTR-mediated apical membrane Cl^- current (I_{Cl}^{apical}) in FRT epithelia heterologously expressing wild-type human CFTR. Figure 8 shows that each loop diuretic (tested at 100 μM) caused a time-dependent attenuation of I_{Cl}^{apical}, blocking ~30% of the control current 20 min after drug addition. As controls, we demonstrated that I_{Cl}^{apical} was unaffected by the Na^+-K^+ ATPase inhibitor ouabain (1 μM), but abolished by the thiazolidinone CFTR inhibitor $CFTR_{inh}$-172 (10 μM) (Ma *et al.*, 2002) (Figure 8). Thus, like glibenclamide (e.g. Sheppard *et al.*, 1994; Li *et al.*, 2004), bumetanide, furosemide, piretanide and xipamide are open-channel blockers that attenuate weakly CFTR-mediated transepithelial Cl^- transport.

Discussion and conclusions

This study investigated how loop diuretics inhibit CFTR and explored structure–activity relationships. We demonstrated that bumetanide, furosemide, piretanide and xipamide are open-channel blockers of CFTR. With distinct kinetics, they impede Cl^- flow by occluding the intracellular vestibule of the CFTR pore.

Comparison of the effects of loop diuretics on NKCCs (SLC12A1 and SLC12A2) (Hebert *et al.*, 2004) and CFTR (ABCC7) highlights similarities and differences in their mechanism(s) of action, as discussed in detail below.

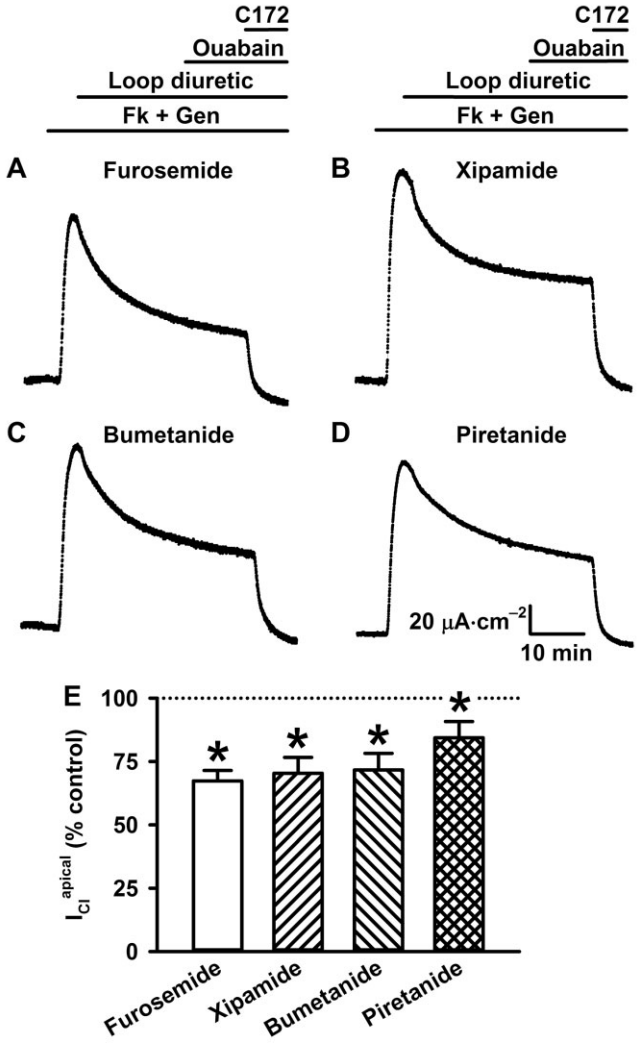

Figure 8

Loop diuretics inhibit apical membrane CFTR Cl^- currents. (A–D) Time courses of I_{Cl}^{apical} in FRT epithelia expressing wild-type human CFTR. During the periods indicated by the bars: (i) forskolin (Fk, 10 μM) and genistein (Gen, 50 μM); (ii) loop diuretics (100 μM); (iii) ouabain (1 μM); and (iv) $CFTR_{inh}$-172 (C172, 10 μM) were present in the apical and basolateral solutions. Prior to the recording, the basolateral membrane was permeabilized with nystatin (0.36 $mg \cdot mL^{-1}$). Transepithelial voltage was clamped at 0 mV and there was a large Cl^- concentration gradient across epithelia (basolateral $[Cl^-]$, 149 mM; apical $[Cl^-]$, 14.8 mM). (E) Effects of loop diuretics on I_{Cl}^{apical}. Values represent I_{Cl}^{apical} measured 20 min after loop diuretic addition normalized to control values recorded immediately before addition and corrected for the spontaneous decay of I_{Cl}^{apical} in the absence of loop diuretics at this time point (34 ± 6%; $n = 6$). Data are means + SEM ($n = 6$, except piretanide where $n = 8$); *$P < 0.05$ versus the control.

Similarities between NKCCs and CFTR

The first similarity is stoichiometry of blockade. For both NKCCs and CFTR, the stoichiometry of loop diuretic blockade is one inhibitor per transport protein (Forbush and Palfrey, 1983; present study).

The second similarity is the state dependence of blockade. Inhibition of NKCCs by loop diuretics requires the simultaneous presence of Na^+, K^+ and Cl^-, suggesting inhibition of active transporters (Forbush and Palfrey, 1983; Hannaert *et al.*, 2002). Similarly, loop diuretics block active CFTR Cl^- channels (Venglarik, 1997; Reddy and Quinton, 1999; present study). The data suggest that loop diuretics access their binding site within the CFTR pore from the open-channel configuration. However, it is possible that loop diuretics might bind this site while the channel is closed because there is evidence that the intracellular vestibule is accessible in the closed-channel configuration (El Hiani and Linsdell, 2010).

The third similarity is competition with Cl^- ions. Early studies suggested that loop diuretics compete directly or indirectly with Cl^- for a common binding site on NKCC1 (Ludens, 1982; Haas and McManus, 1983). Following the molecular identification of NKCC1 (Delpire *et al.*, 1994), the binding sites for Cl^- and bumetanide were localized to the membrane-spanning domain (MSD) of NKCC1 using human–shark chimeric constructs (Isenring and Forbush, 1997). Within this region, residues in transmembrane segment 2 (M2), M4 and M7 determine the difference in Cl^--binding affinity between human and shark NKCC1, whereas residues in M2, M4, M7, M11 and M12 specify the difference in bumetanide binding (Isenring *et al.*, 1998a,b). For CFTR, block by furosemide, but not piretanide, is relieved by inwardly directed Cl^- flow. The simplest interpretation of these data is that furosemide and Cl^- might directly or indirectly compete for a common binding site within the CFTR pore. However, reducing the external Cl^- concentration likely alters electrostatic potentials within the CFTR pore (Liu *et al.*, 2003), complicating data interpretation.

Differences between NKCCs and CFTR

The first difference is the site of blockade. Loop diuretics interact with a site accessible from the extracellular side of the membrane to inhibit NKCCs (Forbush and Palfrey, 1983; Isenring and Forbush, 1997). By contrast, the slow onset of CFTR inhibition when loop diuretics are added to the outside of cells, but the rapid development of blockade in excised membrane patches (Reddy and Quinton, 1999; present study), suggests that loop diuretics access their binding site on CFTR from the intracellular side of the membrane. Consistent with this idea, the voltage dependence of loop diuretic inhibition of CFTR argues that these agents are open-channel blockers that occlude the intracellular vestibule of the CFTR pore (Li and Sheppard, 2009; present study). Moreover, the time dependence of piretanide blockade following a hyperpolarizing voltage step suggests that like glibenclamide (Zhang *et al.*, 2004a), it might interact with multiple sites to prevent Cl^- flow.

The second difference is blocker affinity and rank order of inhibition. Reminiscent of the effects of glibenclamide on pancreatic beta cell ATP-sensitive K^+ channels and CFTR (Inagaki *et al.*, 1995; Sheppard and Robinson, 1997), a notable difference between NKCCs and CFTR is affinity of block. For example, bumetanide inhibits recombinant human NKCC1 with 200-fold greater potency than recombinant human CFTR [NKCC1, $K_{i(bumetanide)}$ = 0.25 μM (Isenring *et al.*, 1998a); CFTR, $K_{i(bumetanide)}$ = 56 μM (excised membrane patches; present study)]. This difference in blocker affinity is

accentuated when CFTR is studied in polarized epithelia (Reddy and Quinton, 1999; present study), arguing that CFTR inhibition is an unlikely consequence of diuretic therapy. Loop diuretics inhibit NKCCs in the rank order: bumetanide > piretanide > furosemide = xipamide with block by bumetanide substantially stronger than that of furosemide (Piyasena *et al.*, 1975; Schlatter *et al.*, 1983; Hannaert *et al.*, 2002). By contrast, loop diuretics inhibit CFTR with little difference in potency (rank order: xipamide ≥ bumetanide = piretanide ≥ furosemide) (present study). Thus, the structural features of loop diuretics, which determine CFTR blockade, are likely to differ from those that confer NKCC inhibition.

The third difference is the voltage dependence of blockade. NKCCs are electroneutral transporters (Haas and Forbush, 2000), suggesting that membrane voltage has little influence on loop diuretics (but, see Paredes *et al.*, 2006). In contrast to NKCCs, anion flow through CFTR is driven by the transmembrane electrochemical gradient, and channel blockade by loop diuretics is voltage dependent (present study). Comparison with other CFTR blockers [e.g. NPPB (Zhang *et al.*, 2000); glibenclamide (Sheppard and Robinson, 1997)] suggests that the anionic form of loop diuretics inhibits CFTR. Consistent with this idea, under the experimental conditions used, the carboxyl moieties of bumetanide, furosemide and piretanide, and the phenolic group of xipamide will all be deprotonated and carry negative charges (Ruiz-Angel *et al.*, 2004).

Structure–activity analysis of NKCC and CFTR inhibition by loop diuretics

Structure–activity studies of NKCC inhibition by loop diuretics suggest that potent NKCC2 inhibition requires a phenyl ring possessing (i) a sulfonamide group at position 5; (ii) an acidic group (e.g. carboxylate) at position 1; (iii) a secondary or tertiary amine at positions 2 or 3 (furosemide, furfurylamine; bumetanide, butylamine; piretanide, pyrrolidine); and (iv) an apolar group at position 4 (furosemide, chloro; bumetanide and piretanide, phenoxy) (Schlatter *et al.*, 1983; Cabantchik and Greger, 1992). Moreover, using NKCC1 structure–function data (Isenring *et al.*, 1998a,b), Hannaert *et al.* (2002) speculated that position 1 interacts with the Cl^- binding site of NKCC1; positions 2 and 3, the cation binding sites, and positions 4 and 5, NKCC1 MSD sequences distinct from the Na^+, K^+ and Cl^- binding sites (see figure 4 of Hannaert *et al.*, 2002).

The present data suggest that the chemical structure of loop diuretics influences the kinetics of CFTR inhibition. Furosemide and xipamide, which possess a chloro group at position 4, block CFTR with 'very fast' speed [residency time ($1/k_{off}$) ~1 ms; see the Supporting Information Results) and block by furosemide is time independent following a hyperpolarizing voltage step. By contrast, bumetanide and piretanide, which carry a phenoxy group at position 4, inhibit CFTR with 'intermediate' speed (piretanide residency time ~6 ms) and inhibition by piretanide is time dependent following a hyperpolarizing voltage step. These data argue that the phenoxy group might slow loop diuretic access to its binding site and stabilize docking within the CFTR pore, possibly through interactions with aromatic residues. We speculate that piretanide, with its larger size and greater lipophilicity, wedges more tightly into the CFTR pore than furosemide (molar volume: piretanide, 256 $cm^3 \cdot mol^{-1}$; furosemide, 206 $cm^3 \cdot mol^{-1}$; polar surface area: piretanide, 181 $Å^2$; furosemide, 131 $Å^2$). This difference might also explain three further distinctions between furosemide and piretanide: (i) the deeper penetration of furosemide into the transmembrane electric field to reach its binding site within the intracellular vestibule of the CFTR pore; (ii) the relief by inwardly directed Cl^- flow of block by furosemide, but not piretanide; and (iii) the asymmetric time dependence of block onset and relief for piretanide, but not furosemide, following voltage steps.

Knowledge of CFTR inhibition by loop diuretics and other open-channel blockers might guide molecular modelling efforts to define the architecture of the intracellular vestibule and identify drug-binding sites within the CFTR pore (Zhou *et al.*, 2001; Linsdell, 2005; St. Aubin *et al.*, 2007; Dalton *et al.*, 2012; Norimatsu *et al.*, 2012a,b). They might also inform the design of innovative small molecule CFTR inhibitors for the treatment of secretory diarrhoea, autosomal dominant polycystic kidney disease and some reproductive disorders (Chan *et al.*, 2009; Li and Sheppard, 2009; Verkman and Galietta, 2009). The widely used open-channel blocker glibenclamide might be used as a framework to engineer higher affinity blockers of the intracellular vestibule. Glibenclamide penetrates deeply into the intracellular vestibule and binds tightly by interacting at multiple sites (Cai *et al.*, 1999; Zhou *et al.*, 2002; Zhang *et al.*, 2004a,b; Dalton *et al.*, 2012). Nevertheless, tighter binding, and hence, higher affinity might be achieved by matching its size to better fit the intracellular vestibule and modifying its charge and/or lipophilicity. Previously, Bachmann *et al.* (1999) reported that two metabolites of glibenclamide hydroxylated at either the 3-*cis* or 4-*trans* positions of the cyclohexyl ring (see Figure 1) had equi- or lower potency than glibenclamide. Because glibenclamide and piretanide inhibit CFTR with similar kinetics, it is unclear whether substitution of the chloro group in glibenclamide by a phenoxy group would enhance further potency, as suggested by the present results. Alternatively, incorporation of additional halide moieties might achieve this goal. In support of this idea, the glycine hydrazide, GlyH-101, the open-channel blocker that occludes the extracellular vestibule by wedging its hydrophobic tail into the pore constriction, possesses two bromo groups (Muanprasat *et al.*, 2004; Norimatsu *et al.*, 2012b). Moreover, phloxine B, a CFTR potentiator that also acts as an open-channel blocker of the intracellular vestibule, possesses multiple halogen groups (Cai and Sheppard, 2002). Identification of the pharmacophore for open-channel blockers that occlude the intracellular vestibule should be a priority for future studies.

In conclusion, CFTR inhibition by furosemide and piretanide resembles block by tolbutamide and glibenclamide. Furosemide and tolbutamide block single channels with 'very fast' speed, and blockade of macroscopic currents is time independent following a hyperpolarizing voltage step (Venglarik *et al.*, 1996; Cui *et al.*, 2012; present study). By contrast, piretanide and glibenclamide block single channels with 'intermediate' speed, and blockade of macroscopic currents is time dependent following a hyperpolarizing voltage step (Sheppard and Robinson, 1997; Cui *et al.*, 2012; present study). Previous work argues that glibenclamide interacts with multiple sites within the intracellular vestibule of the

CFTR pore (Cai *et al.*, 1999; Zhou *et al.*, 2002; Zhang *et al.*, 2004a,b; Dalton *et al.*, 2012). The same is likely the case for loop diuretics, which, with the exception of xipamide, possess both benzenesulfonamide moieties and carboxyl groups, negatively charged side chains predicted to interact with pore-lining residues. In the case of bumetanide and piretanide, their phenoxy group is likely to provide an additional site of interaction to stabilize binding within the intracellular vestibule of the CFTR pore. This locking mechanism is absent in furosemide and xipamide, which lack the phenoxy group. We conclude that differences in molecular dimensions and lipophilicity affect open-channel blockade of CFTR by loop diuretics.

Acknowledgements

We thank HR de Jonge and our departmental colleagues for valuable discussions and MD Amaral, LJV Galietta, CR O'Riordan, Dishman Europe Ltd. and Sanofi-Aventis Deutschland GmbH for generous gifts of cells and small molecules. This work was supported by the Cystic Fibrosis Trust; J. L. was supported by scholarships from the University of Bristol and the Overseas Research Students Awards Scheme of Universities UK and P. K. by the Strategic Scholarships Fellowships Frontier Research Networks, Office of the Higher Education Commission of Thailand.

Conflicts of interest

None.

References

Alexander SPH *et al.* (2013). The Concise Guide to PHARMACOLOGY 2013/14: Overview. Br J Pharmacol 170: 1449–1867.

Bachmann A, Russ U, Quast U (1999). Potent inhibition of the CFTR chloride channel by suramin. Naunyn Schmiedebergs Arch Pharmacol 360: 473–476.

Cabantchik ZI, Greger R (1992). Chemical probes for anion transporters of mammalian cell membranes. Am J Physiol Cell Physiol 262: C803–C827.

Cai Z, Sheppard DN (2002). Phloxine B interacts with the cystic fibrosis transmembrane conductance regulator at multiple sites to modulate channel activity. J Biol Chem 277: 19546–19553.

Cai Z, Lansdell KA, Sheppard DN (1999). Inhibition of heterologously expressed cystic fibrosis transmembrane conductance regulator Cl^- channels by non-sulphonylurea hypoglycaemic agents. Br J Pharmacol 128: 108–118.

Cai Z, Scott-Ward TS, Sheppard DN (2003). Voltage-dependent gating of the cystic fibrosis transmembrane conductance regulator Cl^- channel. J Gen Physiol 122: 605–620.

Cai Z, Taddei A, Sheppard DN (2006). Differential sensitivity of the cystic fibrosis (CF)-associated mutants G551D and G1349D to potentiators of the cystic fibrosis transmembrane conductance regulator (CFTR) Cl^- channel. J Biol Chem 281: 1970–1977.

Cai Z, Li H, Chen J-H, Sheppard DN (2013). Acute inhibition of the cystic fibrosis transmembrane conductance regulator (CFTR) Cl^- channel by thyroid hormones involves multiple mechanisms. Am J Physiol Cell Physiol 305: C817–C828.

Chan HC, Ruan YC, He Q, Chen MH, Chen H, Xu WM *et al.* (2009). The cystic fibrosis transmembrane conductance regulator in reproductive health and disease. J Physiol 587: 2187–2195.

Chen J-H, Cai Z, Sheppard DN (2009). Direct sensing of intracellular pH by the cystic fibrosis transmembrane conductance regulator (CFTR) Cl^- channel. J Biol Chem 284: 35495–35506.

Cui G, Song B, Turki HW, McCarty NA (2012). Differential contribution of TM6 and TM12 to the pore of CFTR identified by three sulfonylurea-based blockers. Pflugers Arch 463: 405–418.

Dalton J, Kalid O, Schushan M, Ben-Tal N, Villà-Freixa J (2012). New model of cystic fibrosis transmembrane conductance regulator proposes active channel-like conformation. J Chem Inf Model 52: 1842–1853.

Delpire E, Rauchman MI, Beier DR, Hebert SC, Gullans SR (1994). Molecular cloning and chromosome localization of a putative basolateral Na^+-K^+-$2Cl^-$ cotransporter from mouse inner medullary collecting duct (mIMCD-3) cells. J Biol Chem 269: 25677–25683.

El Hiani Y, Linsdell P (2010). Changes in accessibility of cytoplasmic substances to the pore associated with activation of the cystic fibrosis transmembrane conductance regulator chloride channel. J Biol Chem 285: 32126–32140.

Farinha CM, Nogueira P, Mendes F, Penque D, Amaral MD (2002). The human DnaJ homologue (Hdj)-1/heat-shock protein (Hsp) 40 co-chaperone is required for the *in vivo* stabilization of the cystic fibrosis transmembrane conductance regulator by Hsp70. Biochem J 366: 797–806.

Forbush B III, Palfrey HC (1983). [^{3}H]Bumetanide binding to membranes isolated from dog kidney outer medulla: relationship to the Na,K,Cl co-transport system. J Biol Chem 258: 11787–11792.

Fuller MD, Thompson CH, Zhang Z-R, Freeman CS, Schay E, Szakács G *et al.* (2007). State-dependent inhibition of cystic fibrosis transmembrane conductance regulator chloride channels by a novel peptide toxin. J Biol Chem 282: 37545–37555.

Gadsby DC, Vergani P, Csanády L (2006). The ABC protein turned chloride channel whose failure causes cystic fibrosis. Nature 440: 477–483.

Gong X, Burbridge SM, Lewis AC, Wong PYD, Linsdell P (2002). Mechanism of lonidamine inhibition of the CFTR chloride channel. Br J Pharmacol 137: 928–936.

Haas M, Forbush B III (2000). The Na-K-Cl cotransporter of secretory epithelia. Annu Rev Physiol 62: 515–534.

Haas M, McManus TJ (1983). Bumetanide inhibits (Na + K + 2Cl) co-transport at a chloride site. Am J Physiol Cell Physiol 245: C235–C240.

Hannaert P, Alvarez-Guerra M, Pirot D, Nazaret C, Garray RP (2002). Rat NKCC2/NKCC1 cotransporter selectivity for loop diuretic drugs. Naunyn Schmiedebergs Arch Pharmacol 365: 193–199.

Hebert SC, Mount DB, Gamba G (2004). Molecular physiology of cation-coupled Cl^- cotransport: the SLC12 family. Pflugers Arch 447: 580–593.

Holland IB, Cole SPC, Kuchler K, Higgins CF (2003). ABC Proteins: From Bacteria to Man. Academic Press: London.

Inagaki N, Gonoi T, Clement JP IV, Namba N, Inazawa J, Gonzalez G *et al*. (1995). Reconstitution of I_{KATP}: an inward rectifier subunit plus the sulfonylurea receptor. Science 270: 1166–1170.

Isenring P, Forbush B III (1997). Ion and bumetanide binding by the Na-K-Cl cotransporter: importance of transmembrane domains. J Biol Chem 272: 24556–24562.

Isenring P, Jacoby SC, Chang J, Forbush B III (1998a). Mutagenic mapping of the Na-K-Cl cotransporter for domains involved in ion transport and bumetanide binding. J Gen Physiol 112: 549–558.

Isenring P, Jacoby SC, Forbush B III (1998b). The role of transmembrane domain 2 in cation transport by the Na-K-Cl cotransporter. Proc Natl Acad Sci U S A 95: 7179–7184.

Kopeikin Z, Sohma Y, Li M, Hwang T-C (2010). On the mechanism of CFTR inhibition by a thiazolidinone derivative. J Gen Physiol 136: 659–671.

Li H, Sheppard DN (2009). Therapeutic potential of cystic fibrosis transmembrane conductance regulator (CFTR) inhibitors in polycystic kidney disease. BioDrugs 23: 203–216.

Li H, Findlay IA, Sheppard DN (2004). The relationship between cell proliferation, Cl^- secretion, and renal cyst growth: a study using CFTR inhibitors. Kidney Int 66: 1926–1938.

Linsdell P (2005). Location of a common inhibitor binding site in the cytoplasmic vestibule of the cystic fibrosis transmembrane conductance regulator chloride channel pore. J Biol Chem 280: 8945–8950.

Liu X, Smith SS, Dawson DC (2003). CFTR: what's it like inside the pore? J Exp Zool 300A: 69–75.

Ludens JH (1982). Nature of the inhibition of Cl^- by furosemide: evidence for competitive inhibition of active transport in toad cornea. J Pharmacol Exp Ther 223: 25–29.

Ma T, Thiagarajah JR, Yang H, Sonawane ND, Folli C, Galietta LJV *et al*. (2002). Thiazolidinone CFTR inhibitor identified by high-throughput screening blocks cholera toxin-induced intestinal fluid secretion. J Clin Invest 110: 1651–1658.

Marshall J, Fang S, Ostedgaard LS, O'Riordan CR, Ferrara D, Amara JF *et al*. (1994). Stoichiometry of recombinant cystic fibrosis transmembrane conductance regulator in epithelial cells and its functional reconstitution into cells *in vitro*. J Biol Chem 269: 2987–2995.

Muanprasat C, Sonawane ND, Salinas D, Taddei A, Galietta LJV, Verkman AS (2004). Discovery of glycine hydrazide pore-occluding CFTR inhibitors: mechanism, structure-activity analysis and in vivo efficacy. J Gen Physiol 124: 125–137.

Norimatsu Y, Ivetac A, Alexander C, Kirkham J, O'Donnell N, Dawson DC *et al*. (2012a). Cystic fibrosis transmembrane conductance regulator: a molecular model defines the architecture of the anion conduction path and locates a 'bottleneck' in the pore. Biochemistry 51: 2199–2212.

Norimatsu Y, Ivetac A, Alexander C, O'Donnell N, Frye L, Sansom MSP *et al*. (2012b). Locating a plausible binding site for an open-channel blocker, GlyH-101, in the pore of the cystic fibrosis transmembrane conductance regulator. Mol Pharmacol 82: 1042–1055.

Paredes A, Plata C, Rivera M, Moreno E, Vázquez N, Muñoz-Clares R *et al*. (2006). Activity of the renal Na^+-K^+-$2Cl^-$ cotransporter is reduced by mutagenesis of *N*-glycosylation sites: role for protein surface charge in Cl^- transport. Am J Physiol Renal Physiol 290: F1094–F1102.

Piyasena KHG, Havard CWH, Weber JCP (1975). Xipamid, a potent new diuretic. Curr Med Res Opin 3: 121–125.

Reddy MM, Quinton PM (1999). Bumetanide blocks CFTR G_{Cl} in the native sweat duct. Am J Physiol Cell Physiol 276: C231–C237.

Riordan JR, Rommens JM, Kerem B-S, Alon N, Rozmahel R, Grzelczak Z *et al*. (1989). Identification of the cystic fibrosis gene: cloning and characterization of complementary DNA. Science 245: 1066–1073.

Ruiz-Angel MJ, Torres-Lapasió JR, García-Alvarez-Coque MC (2004). Effects of pH and the presence of micelles on the resolution of diuretics by reversed-phase liquid chromatography. J Chromatogr A 1022: 51–65.

Russell JM (2000). Sodium-potassium-chloride cotransport. Physiol Rev 80: 211–276.

Schlatter E, Greger R, Weidtke C (1983). Effect of 'high ceiling' diuretics on active salt transport in the cortical thick ascending limb of Henle's loop of rabbit kidney: correlation of chemical structure and inhibitory potency. Pflugers Arch 396: 210–217.

Schmidt A, Hughes LK, Cai Z, Mendes F, Li H, Sheppard DN *et al*. (2008). Prolonged treatment of cells with genistein modulates the expression and function of the cystic fibrosis transmembrane conductance regulator. Br J Pharmacol 153: 1311–1323.

Schultz BD, DeRoos ADG, Venglarik CJ, Singh AK, Frizzell RA, Bridges RJ (1996). Glibenclamide blockade of CFTR chloride channels. Am J Physiol Lung Cell Mol Physiol 271: L192–L200.

Scott-Ward TS, Li H, Schmidt A, Cai Z, Sheppard DN (2004). Direct block of the cystic fibrosis transmembrane conductance regulator Cl^- channel by niflumic acid. Mol Membr Biol 21: 27–38.

Sheppard DN (2004). CFTR channel pharmacology: novel pore blockers identified by high-throughput screening. J Gen Physiol 124: 109–113.

Sheppard DN, Robinson KA (1997). Mechanism of glibenclamide inhibition of cystic fibrosis transmembrane conductance regulator Cl^- channels expressed in a murine cell line. J Physiol 503: 333–346.

Sheppard DN, Carson MR, Ostedgaard LS, Denning GM, Welsh MJ (1994). Expression of cystic fibrosis transmembrane conductance regulator in a model epithelium. Am J Physiol Lung Cell Mol Physiol 266: L405–L413.

St. Aubin CN, Zhou J-J, Linsdell P (2007). Identification of a second blocker binding site at the cytoplasmic mouth of the cystic fibrosis transmembrane conductance regulator chloride channel pore. Mol Pharmacol 71: 1360–1368.

Venglarik CJ (1997). Furosemide and bumetanide block CFTR Cl^- channels. Pediatr Pulmonol Suppl 14: 230.

Venglarik CJ, Schultz BD, DeRoos ADG, Singh AK, Bridges RJ (1996). Tolbutamide causes open channel blockade of cystic fibrosis transmembrane conductance regulator Cl^- channels. Biophys J 70: 2696–2703.

Verkman AS, Galietta LJV (2009). Chloride channels as drug targets. Nat Rev Drug Discov 8: 153–171.

Wang W, Li G, Clancy JP, Kirk KL (2005). Activating cystic fibrosis transmembrane conductance regulator channels with pore blocker analogs. J Biol Chem 280: 23622–23630.

Winter MC, Sheppard DN, Carson MR, Welsh MJ (1994). Effect of ATP concentration on CFTR Cl^- channels: a kinetic analysis of channel regulation. Biophys J 66: 1398–1403.

Woodhull AM (1973). Ionic blockage of sodium channels in nerve. J Gen Physiol 61: 687–708.

Zegarra-Moran O, Romio L, Folli C, Caci E, Becq F, Vierfond J-M *et al*. (2002). Correction of G551D-CFTR transport defect in epithelial monolayers by genistein but not by CPX or MPB-07. Br J Pharmacol 137: 504–512.

Zhang Z-R, Zeltwanger S, McCarty NA (2000). Direct comparison of NPPB and DPC as probes of CFTR expressed in *Xenopus* oocytes. J Membr Biol 175: 35–52.

Zhang Z-R, Cui G, Zeltwanger S, McCarty NA (2004a). Time-dependent interactions of glibenclamide with CFTR: kinetically complex block of macroscopic currents. J Membr Biol 201: 139–155.

Zhang Z-R, Zeltwanger S, McCarty NA (2004b). Steady-state interactions of glibenclamide with CFTR: evidence for multiple sites in the pore. J Membr Biol 199: 15–28.

Zhou Z, Hu S, Hwang T-C (2001). Voltage-dependent flickery block of an open cystic fibrosis transmembrane conductance regulator (CFTR) channel pore. J Physiol 532: 435–448.

Zhou Z, Hu S, Hwang T-C (2002). Probing an open CFTR pore with organic anion blockers. J Gen Physiol 120: 647–662.

Supporting information

Additional Supporting Information may be found in the online version of this article at the publisher's web-site:

http://dx.doi.org/10.1111/bph.12458

Figure S1 Shows overlays of the chemical structures of the four loop diuretics studied.
Figure S2 Uses noise analysis to explore the kinetics of CFTR block by loop diuretics.
Figure S3 Investigates whether loop diuretics are allosteric blockers of CFTR by exploring whether changing the intracellular ATP concentration affects the efficacy of channel block.
Figure S4 Examines whether loop diuretic-blocked channels reopen first before closing on washout of loop diuretic, PKA and ATP from the intracellular solution.
Table S1 Effects of loop diuretics on corner frequencies derived from spectral analysis of CFTR Cl^- currents.
Table S2 Effects of furosemide and piretanide on the open- and closed-time constants of wild-type CFTR.